Multiple-waveguide trapping devices: a 3D-FDTD simulation study

M. M. Rafiee Fanood[1*], G. B. Loozen[1*], E. Schreuder[2] and J. Caro[1]

[1]Department of Imaging Physics, Delft University of Technology, Lorentzweg 1, 2628 CJ Delft, The Netherlands

[2] LioniX International BV, P.O. Box 456, 7500 AL, Enschede, The Netherlands

**contributed equally to this work.*

We present designs of multiple-waveguide traps based on Si_3N_4 waveguides using 3D finite-difference time-domain simulations. Among the sizes simulated, ridge waveguides of cross section 1 μm×90 nm give the best results. The devices have two, four and eight waveguides equally distributed around a 5 μm diameter cylindrical fluidic volume. Trap stiffness values calculated for a 50 nm EV-like particle are 0.02, 1.60 and 3.84 pN/nm/W for a dual-, quad- and octo-waveguide trap, respectively. The results indicate that quad- and octo-waveguide traps, for the same total power, provide stronger and more stable trapping than a dual-waveguide trap for such small bio-particles.

Introduction

Lab-on-a-chip techniques attract strong attention in bio-sensing applications involving analysis of particles. An attractive direction in this field is on-chip integration of optical trapping and Raman spectroscopy, enabling detection and characterization of biological particles such as bacteria, blood cells, extracellular vesicles (EVs), etc.

In this context we have demonstrated a dual-waveguide device based on Si_3N_4/SiO_2 composite waveguides for trapping and Raman spectroscopy of polystyrene beads [1]. The waveguides are transparent in a wide wavelength range, thus allowing the Raman excitation wavelength of 785 nm. It is harder, however, to trap bio-particles than polystyrene beads, due to their low refractive index contrast with respect to aqueous media and since bio-particles such as EVs can be quite small. These circumstances diminish the trapping forces. Moreover, for larger facet separations the dual-waveguide trap has local regions of a strong optical field (hot spots, acting as preferential trappings sites) close to the waveguide facets, which is less ideal. Previously, multi-fiber traps have been used to alleviate this problem[2]. Using multiple fibers both diminishes the hot spots at the facets and provides a stronger trap in the device center as compared to the dual-fiber trap [2].

Here, we propose designs of multiple-*waveguide* traps with enhanced trapping performance for bio-particles as compared to our previous dual-waveguide trap. We use finite-difference time-domain (FDTD) simulations with Lumerical software [3] in designing the traps. We first determined the most suited waveguide structure for optical trapping. We simulated the spatial field distribution of the beam emitted from various waveguides into water and analyzed the beam quality for trapping. Subsequently, we evaluated the trap stability in the center of dual-, quad- and octo-waveguide traps for EV-like particles of diameter in the range 50-100 nm.

Simulated waveguide structures

The waveguides are Si_3N_4 ridges (refractive index n=2.00) embedded in SiO_2 cladding (n=1.45). Waveguide thicknesses are 50, 60,70, 80, 90, 130 and 170 nm, while the

waveguide width is fixed at 1 μm. The simulations are for TM-polarized waveguide modes, meaning that the electrical field is along the *y*-axis in Fig. 1a and for the Raman wavelength 785 nm. The 130 and 170 nm thick waveguides support higher order TM-modes, while the other waveguides are single mode. Here, we only consider the fundamental mode for all waveguides. Fig. 1a shows the fundamental TM-mode for three selected waveguides. As expected, with decreasing thickness the mode becomes less confined in the high index material.

The beams emitted into water (n=1.33) by the three waveguides are shown in Fig. 1b. The colors in the figure indicate ranges of the energy density of the *E*-field (in kJ/m^3), per Watt of power injected into the mode by the source in the simulation. Going from 170 to 130 nm thickness, the emitted beam diverges less, which is accompanied by a weaker decay in the longitudinal direction. This trend is not continued when going to 50 nm thickness, for which the properties of the emitted beam are dominated by the modal lobes outside the high index material. For distances from the facet exceeding 4 μm this leads to a beam with a split tongue character.

From the energy densities we derived the optical force on a small EV-like particle (n=1.37) for the two directions transverse to the beam axis, *i.e.* in the *x*- and *y*-direction, using the formula $\vec{F}(\vec{r}) = \alpha d_{EV}^3 \vec{\nabla}\left|\vec{E}(\vec{r})\right|^2$, where *F* is the force, *E* the electric field, d_{EV} the EV diameter, and α is a constant. The force is linear around the beam axis, meaning that Hooke's law applies. From the force curves we derive the normalized transverse trap stiffness $\kappa_{x(y)}$ in the *x*(*y*)-direction. Fig. 1c shows trap stiffness curves for the *y*-direction as a function of distance to the facet for a 50 nm EV-like particle. The curves hold for 1 Watt offered to the butt coupling between fiber and chip, the efficiency of which applies to a practical device. The butt-coupling efficiency we have applied holds for a fiber with mode field diameter of 5.3 μm. It is assumed that each waveguide is tapered down from its actual thickness to 35 nm at the fiber-waveguide transition, to obtain the optimum efficiency of 0.92 to the fiber. To have a high and weakly decaying κ, while maintaining single mode operation, we have chosen the 90 nm thick waveguide as a building block for multiple-waveguide traps to be simulated.

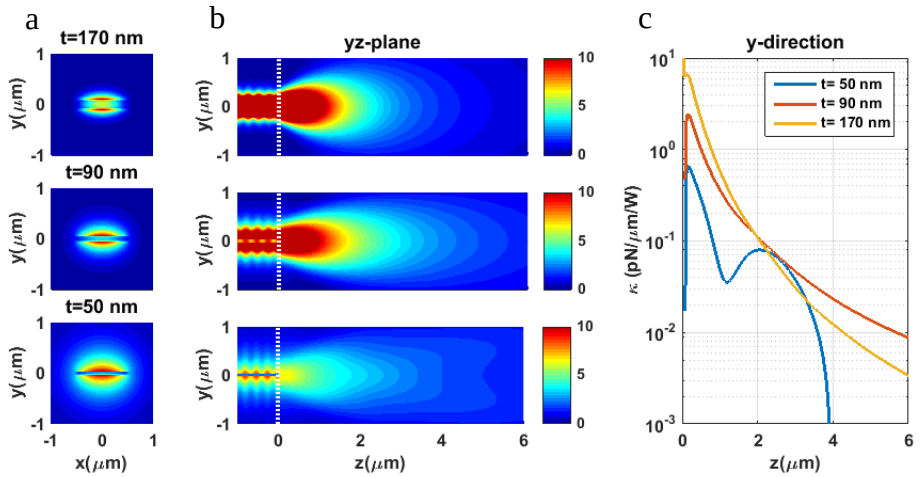

Figure 1. (a) Fundamental TM mode for Si_3N_4 waveguides embedded in SiO_2, for λ=785 nm. Waveguide thickness t as indicated. Waveguide width is 1 μm in each case. (b) Spatial distribution of the beams emitted by the waveguides of (b) into water. The black vertical lines indicate the facet position. (c) Normalized transverse trap stiffness in the *y*-direction for waveguides of thickness t as indicated. Waveguides are tapered down to 35 nm at chip edge for optimum fiber-to-waveguide coupling. Stiffness holds for an EV-like test particle of 50 nm diameter and refractive index 1.37.

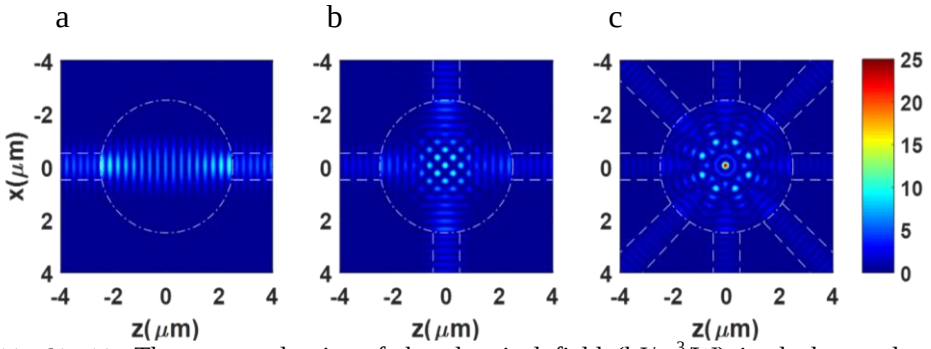

Figure 2. (a), (b), (c): The energy density of the electrical field (kJ/m^3/W) in dual-, quad- and octo-waveguide traps, respectively. The same color scale is used in each case. Boundaries of the waveguides and the fluidic bath are indicated by the dashed lines. Diameter central volume is 5 μm.

Multiple-waveguide traps

We simulated multiple-waveguide traps with two, four and eight waveguides, regularly placed around a 5 μm diameter cylindrical fluidic volume, so as to direct the emitted beams towards the cylinder's center. Waveguides are 1 μm wide and 90 nm thick.

Fig. 2 shows the energy-density distribution for the resulting dual-, quad- and octo-waveguide traps in the central plane. Emitted beams form an interference pattern. Each hot spot of the pattern may act as a local trap for one or more small particle(s). Multiple hot spots acting together may lead to trapping of larger particles. In the dual-waveguide device (a), the local traps in *z*-direction are much narrower than in the other directions, leading to higher intensity gradients and thus stronger local traps in the *z*-direction. Increasing the number of waveguides yields a stronger concentration of light and thus a stronger trap in the device center, as can be seen in the Fig. 2 (b, c). Further, hot spots close to the facets have disappeared for the quad- and octo-waveguide traps, giving a collection of hot spots near the central region.

For these traps, we calculated both the trapping forces and potentials directly from the energy densities in Fig 2. The forces are calculated with the gradient formula above and the potentials, *U*, with the formula $U(\vec{r}) = \alpha d_{EV}^3 \left|\vec{E}(\vec{r})\right|^2$. The above calculations are done for EV-like particles of diameter in the range 50-100 nm as a function of displacement along the *x*-direction for *y= z= 0*. From the resulting force curves, we calculated trap stiffnesses. On the other hand, from the resulting potential curves we determined the minimum optical power P_{min} needed for stable trapping using Ashkin's stability criterion [4]. This states that trapping is stable for $U_o/kT \geq 10$, where U_o is the depth of the trapping potential and *kT* equals 25 meV at room temperature.

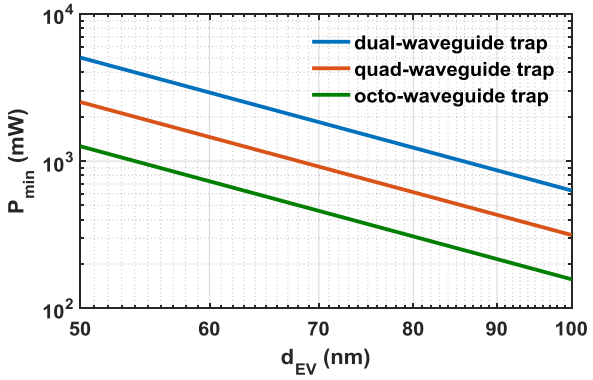

Figure 3. Minimum optical power P_{min} needed to stably trap an EV-like particle as a function of diameter d_{EV}. Colors indicates the different trapping geometries.

These steps finally lead to the straight lines of $P_{\min}$ versus particle diameter d_{EV} in the double logarithmic plot of Fig. 3. The slope of the lines is -3, indicating inverse proportionality with the particle volume, as expected.

We can stably trap the same particle with four-fold lower power by using an octo-waveguide trap rather than dual-waveguide trap. Even more, in the octo-waveguide trap it is possible to stably trap EV-like particles as small as 100 nm with a practical power of 160 mW. The trap stiffness of 50 nm EV-like particle in dual, quad- and octo-waveguide are 0.02, 1.60 and 3.84 pN/nm/W, respectively. These results confirm that a multiple-waveguide trap provides stronger and more stable trap than dual-waveguide trap.

Summary and conclusion

We have proposed designs of multiple-waveguide traps capable of operating at the standard Raman excitation wavelength of 785 nm. Among the waveguides simulated, a rectangular Si_3N_4 ridge waveguide of cross-section 1 μm×90 nm, embedded in SiO_2, gives the best results. All waveguides are thought to be tapered down to 35 nm at the edge of the chip, to achieve the highest fiber-to-waveguide transmission. Multiple-waveguide traps result in stronger and more stable optical trapping in the device center, such that the trap stiffness of a 50 nm EV-like particle increases from 0.02 pN/nm/W for a dual-waveguide trap to 3.84 pN/nm/W in a octo-waveguide trap. This also allows a larger trapping region to accommodate bigger particles. Therefore, the new design is well suited for trapping of bio-particles in the (sub-)micrometer size range. Combining multiple-waveguide traps with a Raman spectrometer enables on-line measuring of bio-particles of which the monitoring and determination of properties are relevant for safe drinking water and diagnosis of diseases in man.

Acknowledgement

This work is part of the research programmes MEMPHISII and Cancer-ID, with project numbers 13531 and 14197, respectively, which are financed by the Netherlands Organisation for Scientific Research (NWO). The simulation work was carried out on the Dutch national supercomputer Cartesius with the support of SURF Cooperative. The use of supercomputer facilities was sponsored by NWO Exact and Natural Sciences.

References

[1] M. Boerkamp, T. van Leest, J. Heldens, A. Leinse, M. Hoekman, R. Heideman, and J. Caro, "On-chip optical trapping and Raman spectroscopy using a TripleX dual-waveguide trap" Optics express vol. 22, 30528-30537, 2014.

[2] S. D. Collins, R. J. Baskin and D. G. Howitt, "Microinstrument gradient-force optical trap," Applied Optics vol.38, 6068-6074, 1999.

[3] Lumerical FDTD Solutions, Inc., http://www.lumerical.com/tcad-products/fdtd/

[4] A. Askin, J. M. Dziedzic, J. E. Bjorkholm and S. Chu, "Observation of single-beam gradient force optical trap for dielectric particles" Opt. Lett. vol. 11, 288–290, 1986.